ELSEVIER

European Polymer Journal 38 (2002) 1071–1078

EUROPEAN POLYMER JOURNAL

www.elsevier.com/locate/europolj

Flow birefringence of temporary polymer networks

D. Chassapis [a,*], A. Balouktsis [a], T.D. Karapantsios [b]

[a] Department of Mechanical Engineering, Technological Educational Institution of Serres, End of Magnesia's Str., GR-62100 Serres, Greece

[b] Chemical Technology Division, Department of Chemistry, Aristotle University of Thessaloniki, Box 116, 54006 Thessaloniki, Greece

Received 27 July 2001; received in revised form 1 October 2001; accepted 8 October 2001

Abstract

The statistical theory of temporary polymer networks is an effort of describing the macroscopic behavior of such networks based on molecular behavior analysis. The calculation of the stress tensor of a network and the satisfactory comparison with experimental viscosity results was shown before [Rheol. Acta 28 (1989) 193]. Here we present the foresights of the theory as regards flow birefringence. The polarizability tensor is calculated first and then the birefringence of a four-functional temporary polymer network is estimated for a stationary simple shear flow. The dependence of the calculated quantities on shear rate is in line with existing experimental evidence.

Keywords: Temporary polymer networks; Magnitude of birefringence; Extinction angle

1. Introduction

A temporary polymer network, i.e. a network whose junctions form and decay, shows increased mobility compared with a permanent network in which the junctions are fixed. Kroener and Takserman-Krozer ([2]) developed a molecular-statistical theory of temporary polymer networks in solution in order to describe quantitatively the dynamic behavior of such a network. It must be mentioned that the extra mobility of the network gives rise to a viscoelasticity, which is nonlinear [1,2].

The result of the above theory was the formulation of the generalized Kirkwood diffusion equation—an integro-differential equation [2]. The diffusion equation was treated within the relaxation time approach, so it became a (high-dimensional) differential equation

$$\frac{\partial W}{\partial t} + \sum_{i}^{M} \nabla_i \cdot (\dot{\vec{r}}_i W) = -\bar{p}(W - W_{\mathrm{eq}}) \qquad (1)$$

where

- $W = W(\vec{R}, Z, M, t)$ is the nonequilibrium probability density function for the state $[\vec{R}, Z, M]$ at time t. W changes in time because, (i) the network flows (left-hand side of Eq. (1)) and (ii) because junctions deform and decay (right-hand side of Eq. (1)).
- $\vec{R} = \{\vec{r}_i\}$ $(i = 1,2, \ldots M)$ is the configurational position vector for the junctions.
- $Z = \{z_{ij}\}$ denotes the chains connecting the neighboring junctions i and j. In the model (four-functional network) there are M junctions and $2M$ chains connecting them.
- M is the number of junctions per volume V.
- W_{eq} is the equilibrium probability density function.
- $\bar{p} = \bar{p}(\vec{R}, Z) \equiv \int\int p(\vec{R}, Z \to \vec{R}', Z')\, \mathrm{d}\vec{R}'\, \mathrm{d}Z'$ is the probability per unit time that the configuration $(\vec{R}, Z)$ will decay into any other configuration.
- $\dot{\vec{r}}_i$ is the velocity of the ith junction, obeying a Langevin equation as given in Refs. [2,3]. The forces included in this equation are the elastic forces (transmitted through the chains), the frictional forces between polymer and solvent and the statistical entropy forces of Brownian motion.

* Corresponding author. Fax: +00-30-321-49128.
E-mail address: dcasap@teiser.gr (D. Chassapis).

0014-3057/02/$ - see front matter
PII: S0014-3057(01)00284-1

Assuming that (i) the density of decay processes is not too high in space and time and (ii) we can replace $\bar{p}(\vec{R}, Z)$ with $\bar{p}(\langle\vec{R}\rangle_{eq}, Z)$ where the brackets $\langle\ \rangle$ denote the ensemble average, the stress tensor $\underline{\underline{\pi}}$ of the network was calculated [2,4], which according to Giesekus [5] is given by the relation

$$\underline{\underline{\pi}} = \frac{N_A c}{M} \sum_{i'}^{M} \lambda_{i'} \langle \vec{s}_{i'}, \vec{s}_{i'} \rangle_S \tag{2}$$

where

- N_A is the Avogadro–Loschmidt number.
- c is the mass concentration of the polymer.
- M is the molecular weight of the polymer.
- $\lambda_{i'}$ are the eigenvalues of the elastic matrix κ, whose elements κ_{ij} are functions of the spring constants k_{ij} of the chain connecting the junctions i and j [4]. For a linearized elasticity they are given from a known formula of Volkenstein [6] and Flory [7].
- $\vec{s}_i$ are the eigenvectors belonging to the vibrating system of junctions and elastic springs between them.
- $\langle \vec{s}_{i'} \vec{s}_{i'} \rangle_S$ are the so-called second moments in the mode representation of the vibrating molecular network. Their calculation was done by a standard procedure from the diffusion equation, after this equation was transformed to normal modes [1,2,4].

The numerical processing of these equations was done by an extensive computer program [4]. The calculated forms for the simple shear flow viscosity functions $\eta \equiv \pi_{xz}/q$ and $\xi \equiv (\pi_{zz} - \pi_{xx})/q^2$, where q is the shear rate, were found to satisfactorily describe the experimental data. This concerned both the stationary [3,4] and the nonstationary flow [1] of polystyrene solution in toluene. The quantitative agreement between model predictions and experimental observations was considered as evidence of the accurate theoretical estimation of $\underline{\underline{\pi}}$ for that polymeric system.

In the present paper we show that the aforementioned theory gives good results also for the birefringence values and the extinction angle of temporary polymer networks in steady shear flow. This is so because the decisive parameter for the determination of these quantities is once more the stress tensor $\underline{\underline{\pi}}$ of the network (see later). Indeed, it is rather common knowledge that birefringence is directly related to viscosity [12]. On the other hand, the calculation of $\underline{\underline{\pi}}$ is also the major shortcoming of the theory since it requires *simultaneous* knowledge of the limiting viscosity functions $\eta_0 = \lim_{q\to 0} \eta$ and $\xi_0 = \lim_{q\to 0} \xi$. At present these quantities are not trivial to obtain and for this reason they are not available for most polymeric solutions. This fact greatly diminishes the extent of usable experimental data to compare with.

2. Basic conceptions

One of the most commonly used methods for exploring the molecular structure in liquids is the study of birefringence which the liquid exhibits under an external electric or magnetic field. However, concerning the case of a polymer with flexible macromolecules the above method is not effective [8]. When birefringence is induced via mechanical forces like the shear stresses in a laminar flow (''Maxwell-dynamo-optic effect'') the situation is substantially different. Such a flow birefringence of a polymer solution is a function of the geometrical, mechanical and optical properties of the solute macromolecules [9,10,11,12]. It is apparent that flow birefringence can provide direct information about dimensions and structure of the macromolecules.

The birefringence values are defined as the differences between the principal refractive indexes n_1, n_2 and n_3:

$$\Delta_1 \equiv n_2 - n_3 \tag{3}$$

$$\Delta_2 \equiv n_3 - n_1 \tag{4}$$

$$\Delta_3 \equiv n_1 - n_2 \tag{5}$$

It can be seen that only two of the above quantities are independent of each other since $\Delta_3 = -\Delta_2 - \Delta_1$. Especially in the case of a coaxial specimen (i.e. a specimen for which the orientation of the structural elements shows a cylindrical symmetry around a characteristic direction), two of the principal refractive indexes are equal to each other. Thus, a single value of birefringence can describe the specimen's birefringence.

The relation between the refractive index and specific polarizability P (polarizability of the unit volume) can be described by the well known Lorentz–Lorentz law of classical electrodynamics. This relation rigorously applies only to perfectly isotropic materials but has been extensively used also in the field of polymeric solutions as an adequate approximation, [10,11]. This is because most of polymeric solutions behave isotropically under small shear rates. This equation is:

$$\frac{n^2 - 1}{n^2 + 2} = \frac{4\pi}{3} P \tag{6}$$

Differentiation of Eq. (6) results in [13]:

$$\frac{6n}{(n^2 + 2)^2} \mathrm{d}n = \frac{4\pi}{3} \mathrm{d}P \tag{7}$$

If the difference between the principal refractive indexes is small enough we can replace $\mathrm{d}n$ and $\mathrm{d}P$ in Eq. (7) by Δn and ΔP, respectively. Then Eq. (7) becomes, for instance,

$$\Delta_2 \equiv n_3 - n_1 = \frac{2\pi}{9}\frac{(n^2+2)^2}{n}(P_3 - P_1) \tag{8}$$

Eq. (8) gives the dependence of birefringence on the corresponding difference of specific polarizability. In this equation, n is the usual refractive index of the nonfatigued material.

The anisotropy of polarizability is related to the anisotropic distribution of structural elements, which are also anisotropic. Below we present the derivation of a quantitative expression for the anisotropy of polarization in the case of a four-functional polymer network.

3. Polarizability tensor of a four-functional polymer network

We consider a four-functional network [2,4], consisting of junctions M and $2M$ chains. The two polarizability components, $\gamma_{ij}^{\parallel}$ and $\gamma_{ij}^{\perp}$, of a ij chain, parallel and perpendicular to the end-to-end vector $\vec{h}_{ij} = \vec{r}_j - \vec{r}_i$, are given by the equations [14]:

$$\gamma_{ij}^{\parallel} = g + 2f_{ij}h_{ij}^2 \tag{9}$$

$$\gamma_{ij}^{\perp} = g - f_{ij}h_{ij}^2 \tag{10}$$

where

$$g = \frac{N}{3}(\alpha_1 + 2\alpha_2) \tag{11}$$

$$f_{ij} = \frac{1}{5}\frac{(\alpha_1 - \alpha_2)}{5\langle h_{ij}^2\rangle_{\mathrm{eq}}} \tag{12}$$

In the above equations

- α_1 and α_2 are the polarizability components parallel and perpendicular to the statistical "Kuhn-segments". According to the above, it must be particularly stressed that while it is allowed for the statistical segments to have different lengths, it is also presupposed that all segments have the same anisotropy $(\alpha_1 - \alpha_2)$. So, the magnitude $(\alpha_1 - \alpha_2)$ becomes a very important microstructural characteristic of the polymer. It could be argued that the difference $(\alpha_1 - \alpha_2)$ represents an estimated mean value for all the statistical segments. The magnitude $(\alpha_1 - \alpha_2)$ has been already experimentally determined for a series of polymers, [15].
- N is the number of statistical segments from which a macromolecule is constituted. It has an unknown magnitude but this is not a problem because it does not appear in the final result.
- $\langle h_{ij}^2\rangle_{\mathrm{eq}}$ represents the mean value of the end-to-end vector's square in equilibrium (relaxing fluid).

According to Eqs. (9)–(12) the polarizability tensor $\underline{\underline{\gamma}}_{ij}$ of the chain ij is given (in regular form) from the following relation:

$$\underline{\underline{\gamma}}_{ij} = \left(g - f_{ij}h_{ij}^2\right)\underline{\underline{I}} + 3f_{ij}\begin{pmatrix} 0 & 0 & 0 \\ 0 & 0 & 0 \\ 0 & 0 & h_{ij}^2 \end{pmatrix} \tag{13}$$

where $\underline{\underline{I}}$ is the unitary tensor.

The polarizability tensor $\underline{\underline{P}}$ of the whole four-functional network arises by summing the polarizabilities of all chains:

$$\underline{\underline{P}} = \sum_{(ij)}^{2M}\underline{\underline{\gamma}}_{ij} = \frac{1}{2}\sum_{i}^{M}\sum_{\alpha}^{4}\underline{\underline{\gamma}}_{i\alpha} \tag{14}$$

If we bring the polarizabilities $\underline{\underline{\gamma}}_{ij}$ and $\underline{\underline{\gamma}}_{i\alpha}$ to a Cartesian coordinates system (x, y, z) and calculate the mean value P of the polarizability tensor $\underline{\underline{P}}$, we end up with:

$$\begin{aligned} P &\equiv \langle\underline{\underline{P}}\rangle \\ &= M\left(g - f_{ij}\right)\underline{\underline{I}} + 3f\begin{pmatrix} \langle\underline{x}^{\mathrm{T}}\kappa\underline{x}\rangle & \langle\underline{x}^{\mathrm{T}}\kappa\underline{y}\rangle & \langle\underline{x}^{\mathrm{T}}\kappa\underline{z}\rangle \\ \langle\underline{y}^{\mathrm{T}}\kappa\underline{x}\rangle & \langle\underline{y}^{\mathrm{T}}\kappa\underline{y}\rangle & \langle\underline{y}^{\mathrm{T}}\kappa\underline{z}\rangle \\ \langle\underline{z}^{\mathrm{T}}\kappa\underline{x}\rangle & \langle\underline{z}^{\mathrm{T}}\kappa\underline{y}\rangle & \langle\underline{z}^{\mathrm{T}}\kappa\underline{z}\rangle \end{pmatrix} \end{aligned} \tag{15}$$

$$\text{where} \quad f = \frac{1}{15}\frac{(\alpha_1 - \alpha_2)}{k_{\mathrm{B}}T}, \tag{16}$$

k_{B} is the Boltzmann's constant and T is the absolute temperature.

When deriving Eq. (15), it is assumed that all mean values $\langle h_{ij}^2\rangle_{\mathrm{eq}}$ are equal for all chains (due to the isotropy of the polymer network in the equilibrium state). In Eq. (15) the following formalism is used:

$$\underline{x} = \begin{pmatrix} x_1 \\ x_2 \\ \vdots \\ x_M \end{pmatrix}, \qquad \underline{y} = \begin{pmatrix} y_1 \\ y_2 \\ \vdots \\ y_M \end{pmatrix}, \qquad \underline{z} = \begin{pmatrix} z_1 \\ z_2 \\ \vdots \\ z_M \end{pmatrix} \tag{17}$$

It must be noted that Eq. (15) is in qualitative agreement with Zimm's relation [16,17], which however, is valid for very dilute solutions, where the polymer is in isolated macromolecules form. The apparent resemblance between Eq. (15) and other equations derived in the past for polymer solutions and networks is due to the similar derivation procedures which are, virtually, alternatives of the same "spring and bead model" [5,17]. That is, all studies start from the equations of Kuhn and Gruen (Eqs. (9)–(12); [14]) which describe the polarizabilty components of a single chain and after summing up over all possible springs obtain the total polarizabilty of the network. The present analysis manages to explicitly incorporate in Eq. (15) the elastic matrix (κ), characteristic of a four-functional network without open ends. This matrix does not only describe the topology of the

network, as for instance Zimm's relation does, but also determines quantitatively the elastic forces between junctions i and j through a chain ij [4]. So, Eq. (15) demonstrates on a microscopic scale how birefringence is induced via mechanical forces like the shear stresses in a laminar flow (''Maxwell-dynamo-optic-effect'').

Eq. (15) is going to be used in conjunction with Eq. (8) to determine the birefringence and extinction angle values. Next, we will show the significance of the above relation in the case of a simple shear flow.

4. Flow birefringence in simple shear flow

The case of a laminar flow described by a velocity gradient tensor has the following form in Cartesian coordinates:

$$\underline{\underline{q}} = q \begin{pmatrix} 0 & 0 & 1 \\ 0 & 0 & 0 \\ 0 & 0 & 0 \end{pmatrix} \tag{18}$$

According to the above, characterized as simple shear flow the z-axis coincides with the flow direction, while the x-axis coincides with the velocity gradient direction. Then, as it is customary for birefringence experiments, the y-axis is the observation direction.

During an experimental procedure, the refractive indexes difference $\Delta n = n_3 - n_1$ of the specimen is of interest. Here, n_3 and n_1 are the refractive indexes for a parallel and a perpendicular to the optical axis polarized ray respectively. The corresponding difference ΔP between the fundamental polarizabilities, which, according to Eq. (8), determines the birefringence value, arises from table diagonalisation in Eq. (15):

$$\Delta P = 3f\sqrt{\left[\left(\langle \underline{z}^{\mathrm{T}} \kappa \underline{z}\rangle - \langle \underline{x}^{\mathrm{T}} \kappa \underline{x}\rangle\right)^2 + 4\langle \underline{z}^{\mathrm{T}} \kappa \underline{x}\rangle^2\right]} \tag{19}$$

Inserting, in the above, the extinction angle (χ) (which is the smallest angle between flow direction and optical axis), yields:

$$\tan 2\chi = \frac{2\langle \underline{z}^{\mathrm{T}} \kappa \underline{x}\rangle}{\langle \underline{z}^{\mathrm{T}} \kappa \underline{z}\rangle - \langle \underline{x}^{\mathrm{T}} \kappa \underline{x}\rangle} \tag{20}$$

After some elementary algebra, the relation for ΔP becomes:

$$\Delta P = 3f\frac{2\langle \underline{z}^{\mathrm{T}} \kappa \underline{x}\rangle}{\sin 2\chi} \tag{21}$$

By substituting Eq. (21) in Eq. (8) the following arises for the value of birefringence:

$$\Delta n = \frac{4\pi}{45k_{\mathrm{B}}T}\frac{(n^2+2)^2}{n}(\alpha_2 - \alpha_1)\frac{N_{\mathrm{A}}c}{M}\frac{\langle \underline{z}^{\mathrm{T}} \alpha \underline{x}\rangle}{\sin 2\chi} \tag{22}$$

For the derivation of Eqs. (20) and (22) the only assumption is about the isotropy of the network which leads to a progressively poorer accuracy as the shear rate increases. Apart from that, the accuracy of predictions is satisfactory inasmuch as the model of a four-functional temporary polymer network describes adequately the actual behavior of polymer solutions. There is evidence that this is the case for moderate polymer concentrations as those employed in the present study [1,4].

In order to include some physically meaningful variables in Eqs. (20) and (22), a further transformation is performed. The stress tensor $\underline{\underline{\pi}}$ of a polymer network is given by the following relation [4]:

$$\underline{\underline{\pi}} = \frac{N_{\mathrm{A}}c}{M}\langle \underline{R}^{\mathrm{T}} \kappa \underline{R}\rangle \tag{23}$$

$$\text{where} \quad \underline{R} = \begin{pmatrix} \underline{r}_1 \\ \underline{r}_2 \\ \vdots \\ \underline{r}_M \end{pmatrix} \tag{24}$$

$\underline{r}_i$ $(i = 1, 2, \ldots M)$ is the position vector of junction i. Using the above relations and after some elementary considerations we can rewrite Eqs. (20) and (22) in the following form:

$$\tan 2\chi = 2\frac{\pi_{xz}}{\pi_{zz} - \pi_{xx}} \tag{25}$$

$$\Delta n = \frac{4\pi}{45k_{\mathrm{B}}T}\frac{(n^2+2)^2}{n} \times (\alpha_1 - \alpha_2)\sqrt{(\pi_{zz} - \pi_{xx})^2 + (2\pi_{xz})^2} \tag{26}$$

Eqs. (25) and (26), can be viewed as a realization of the ''photoelastic stress analysis''. A meticulous survey of the pertinent literature reveals that the available experimental data on the limiting viscosity functions, η_0 and ξ_0, for polymer networks is scanty. This is more so if one requires knowledge of both functions for the same material. As a matter of course, either one of η_0 or ξ_0 is known for most materials. Furthermore, we were not able to locate even a single polymer solution for which both the limiting viscosity functions and also data on flow birefringence or extinction angle are available. On this account, it was decided to proceed by comparing the theoretical predictions for a system of known rheology against experimental birefringence and extinction angle data for other polymeric systems. The foundation for doing so is that polymer networks of ordinary (statistical) degrees of functionality are quite prone to a similar qualitative molecular behavior under simple shear flow [4].

Eqs. (25) and (26) are employed next to investigate the case of a polystyrene solution in toluene for different mass concentrations and molecular weights of the polymer. To do so, the required components of the stress tensor are taken from [4]. The results are presented

in Figs. 1–4. In Figs. 1 and 3, comparisons are made against experimental evidence of Δn and χ for other polymer solutions that has been very recently presented in literature, Table 1. The use of modern instrumentation by those studies allows confidence regarding the reliability of measurements. The typical experimental

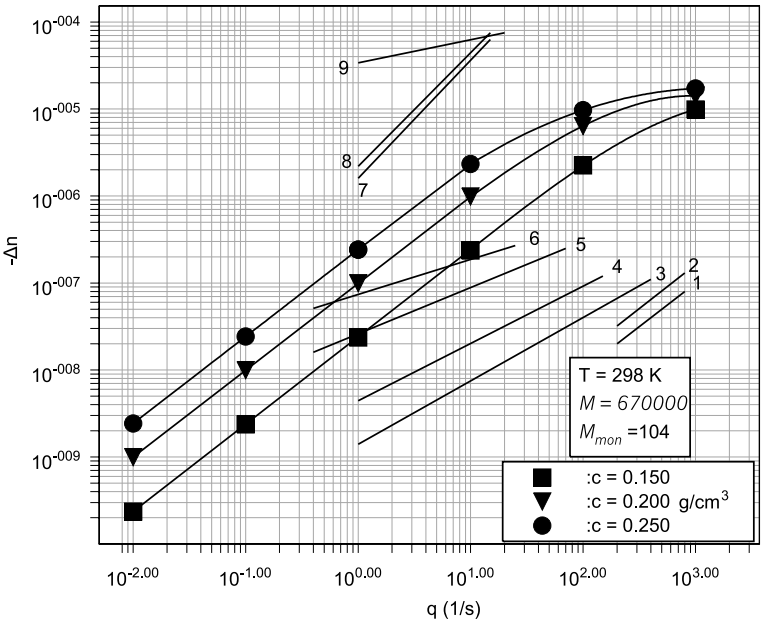

Fig. 1. Estimated birefringence value (Δn) vs shear rate (q) for a simple shear flow of a 15%, 20% and 25% solution of polystyrene in toluene ($M = 670000$). Numbered lines refer to data sets in Table 1.

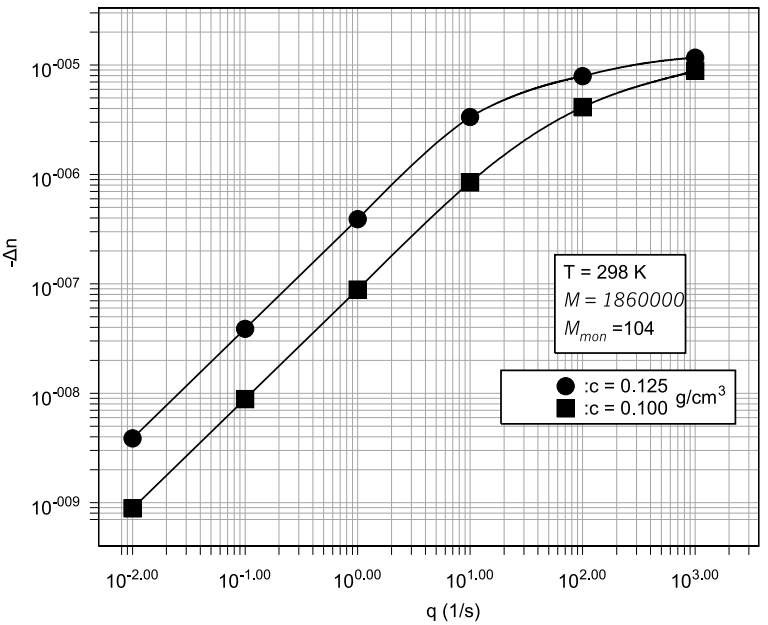

Fig. 2. Estimated birefringence value (Δn) vs shear rate (q) for a simple shear flow of a 10%, and 12.5% solution of polystyrene in toluene ($M = 1860000$).

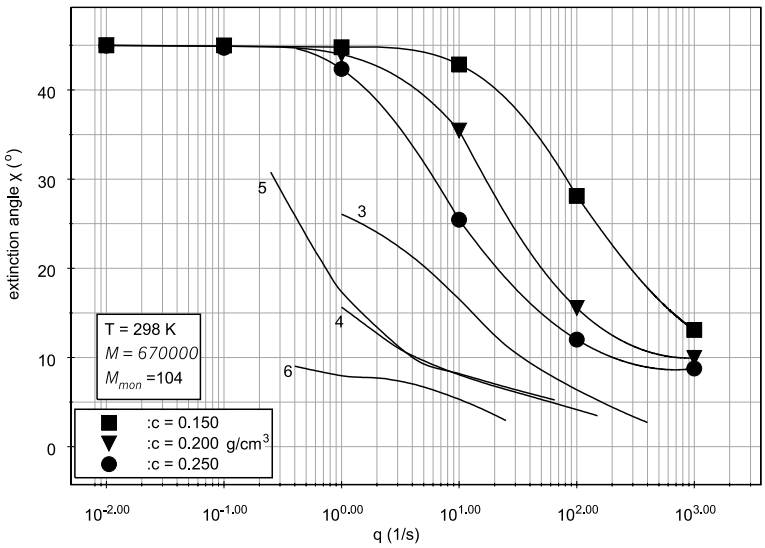

Fig. 3. Estimated extinction angle (χ) vs shear rate (q) for a simple shear flow of a 15%, 20% and 25% solution of polystyrene in toluene ($M = 670000$). Numbered lines refer to data sets in Table 1.

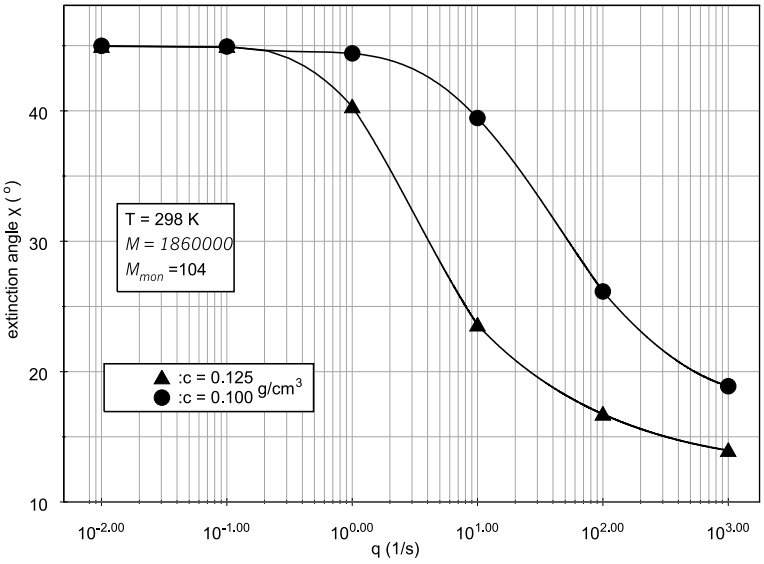

Fig. 4. Estimated extinction angle (χ) vs shear rate (q) for a simple shear flow of a 10%, and 12.5% solution of polystyrene in toluene ($M = 1860000$).

error in such measurements is around 10% [12]. These data span a wide variety of materials of different molecular weight, concentration and character (solutions, melts) and exhibit a positive birefringence. For clarity in the presentation, past data in Figs. 1and 3 are shown in the form of best-fit lines through measurements (statistically confident to 95% level).

For very small shear rates, $q \ll 10^{-2}$ s^{-1}, the birefringence Δn, equals practically to zero ($< 10^{-9}$) (Figs. 1 and 2), and the extinction angle χ is approximately 45° (Figs. 3 and 4). These values obtained at very small q manifest the isotropy of the network in the relaxation state. Affinity for such small values have been repeatedly observed in past experiments for several polymeric networks, e.g. Refs. [18–20]. The same behavior was reported also in earlier studies, e.g. Refs. [8,17,21]; and is an essential initial condition for the successful performance of any theoretical model.

Table 1
Recent experimental studies in literature with which the present theory is compared

Data set	Reference	Polymer solution or melt	M	c
1	[19]	Copolymers of *para*- and *meta*-phenylene-1,3,4-oxadiazoles (weight part of m-units = 0.33) in sulfuric acid	25 000–33 000	0.00031 g cm^{-3}
2	[19]	Copolymers of *para*- and *meta*-phenylene-1,3,4-oxadiazoles (weight part of m-units = 0.33) in sulfuric acid	25 000–33 000	0.0005 g cm^{-3}
3	[20]	Poly(methylmethacrylate) in toluene	10 600 000	2 wt.%
4	[20]	Poly(methylmethacrylate) in toluene	19 200 000	2 wt.%
5	[20]	Poly(methylmethacrylate) in *N*,*N*-dimethylformamide	10 600 000	2 wt.%
6	[20]	Poly(methylmethacrylate) in *N*,*N*-dimethylformamide	19 200 000	2 wt.%
7	[18]	Linear metallocene linear low density polyethylene (LLDPE) (melt)	100 000	–
8	[18]	20% Linear metallocene LLDPE + 80% long chain-branched metallocene LLDPE (melt)	100 000	–
9	[18]	Long chain-branched metallocene LLDPE (melt)	100 000	–

At a fixed shear rate (q) and molecular weight (M), Δn increases with increasing mass concentration (c) (Figs. 1 and 2). The same trend is observed in data sets 1 and 2 [19] and is also reported by Pavlov et al. [12]. In addition, at a fixed shear rate and mass concentration, it can be easily inferred from the same figures that Δn increases also with molecular weight. The same behavior is acknowledged by data sets 3, 4, 5 and 6 [19]. The opposite trends are observed for the extinction angle (Figs. 3 and 4). On the whole, such trends are rather expected on physical grounds and are in line with experiments conducted with other polymeric solutions [12,19].

Already for $q \geqslant \sim 10^{-2}$ and up to $q \leqslant \sim 10^{2}$ s^{-1}, Δn increases linearly with respect to q due to the progressively increasing orientation of the network chains. This is displayed in the log–log plots of Figs. 1 and 2 and is in accord with experimental results for other polymer networks [18–20]. The lower the mass concentration of the polymer the higher the shear rate value up to where the linear behavior is valid.

The extinction angles decay in a monotonous fashion, too (Figs. 3 and 4). However, the shape of the χ curves differs from the Δn curves as expected from Eq. (25). As with Δn, the experimental data shown in Fig. 3 have certain features in common with predictions. They decay monotonously with q within a comparable range of values and at comparable rates.

For very large shear rates ($q \geqslant 10^{3}$ s^{-1}) a saturation state is predicted, independent from mass concentration and molecular weight, at least for the examined range of parameters. This is clearly manifested by the gradual leveling-off of both Δn and χ predictions towards somewhat constant values. This is in qualitative accordance with recent experiments displayed in Fig. 3 [20], where especially for χ the measurements present a progressive leveling-off as q increases. Earlier evidence by Fuller and Leal [21], showed also a similar behavior.

5. Conclusions

This work provides evidence that the molecular-statistical theory originally developed by Kroener and Takserman-Krozer [2] constitutes a useful tool for estimating the birefringence and extinction angle of a four-functional temporary polymer network under simple shear flow. Estimations are based on the stress tensor calculated from the above theory and an appropriate expression derived for the polarizability tensor of the network. At present, the lack of information in literature as regards certain limiting viscosity data necessary to calculate the stress tensor of polymeric solutions, hampers the rigorous quantitative assessment of the model predictions against experimental data for the same material. Yet, the qualitative agreement between the experimentally observed behavior and model predictions for different polymer networks is a strong indication that the model has the potential to satisfactorily describe the phenomena occurring in these networks. The most profound of these features are the dependence of birefringence and extinction angle on molecular weight and concentration, the linear increase of birefringence with shear rate for an intermediate range of shear rates ($\sim 10^{-2}$ s^{-1} $< q <$ $\sim 10^{2}$ s^{-1}) and the tendency for a gradual saturation at much higher shear rates ($q \geqslant 10^{3}$ s^{-1}).

References

[1] Chassapis D, Babos G, Takserman-Krozer R, Kroener E. Rheol Acta 1989;28:193–201.
[2] Kroener E, Takserman-Krozer R. Rheol Acta 1984;23:1–9 and 139–50.
[3] Kroener E, Chassapis D, Takserman-Krozer R. The physics of temporary polymer networks. In: Kramer O, editor. Biological and synthetic polymer networks. London: Elsevier; 1988. p. 185–205.
[4] Chassapis D. Zur molekular-statistischen Theorie temporaerer Polymernetzwerke-Theoretische Untersuchungen und Vergleich mit Experimenten. PhD Dissertation, University of Stuttgart, 1986.
[5] Bird BR, Hassager O, Armstrong RC, Curtis CHF. In: Dynamic of polymeric liquids, vol. 2. New York: Wiley; 1977 [Chapter 13].
[6] Volkenstein MV. In: Configurational statistics of polymer chains. New York: Interscience; 1963.
[7] Flory PJ. Statistical mechanics of chain molecules. New York: Interscience; 1969.
[8] Tsvetkov VN. Polym Rev 1964;6:563–85.
[9] Janeschitz-Kriegl H. Polymer melt rheology and flow birefringence. Berlin: Springer; 1983.
[10] Fuller GG. Optical rheometry of complex fluids. New York: Oxford University Press; 1995.
[11] Li J-M, Burghardt RW, Yang B, Khonami B. J Non-Newton Fluid Mech 2000;91:189–220.
[12] Pavlov GM, Kolbina GF, Shtennikova IN, Michailova NA, Korneeva EV. Eur Polym J 2001;37:1219–25.
[13] Stein RS. Polym Rev 1964;6:155–63.
[14] Kuhn W, Gruen F. Kolloid Zeitschrift 1942;101(Heft 3): 249–71.
[15] Brandrup J, Immergut EH, editors. Polymer handbook. New York: Wiley; 1966.
[16] Zimm BH. J Chem Phys 1956;24:269–78.
[17] Yamakawa H. Modern theory of polymer solutions. New York: Harper and Row Publication; 1971.
[18] Chai CK, Creissel J, Randrianantroandro H. Polymer 1999;40:4431–6.
[19] Lavrenko PN, Strelina IA, Okatova OV, Shulz B. Eur Polym J 2000;36:1927–32.
[20] Dell'Erba R. Polymer 2001;42:2655–63.
[21] Fuller GG, Leal LG. Rheol Acta 1980;19:580–600.